

Investigation of vehicle – bridge interaction for highway bridges

R. CANTIENI, *Dr sc techn*, ETH, Head, Concrete Structures Section, EMPA, Swiss Federal Laboratories for Materials Testing and Research, Switzerland

Experience shows that bridges with fundamental natural frequencies in the range $f = 2.0 \dots 4.0$ Hz respond more strongly to the dynamic action of heavy commercial traffic than other bridges [1]. To achieve better insight into the processes occurring during the passage of a vehicle over a highway bridge with a critical natural frequency dynamic load tests have been performed. The parameters "natural behavior of the bridge" and "longitudinal pavement profile" have been carefully determined before the tests. During the tests the dynamic wheel loads were measured as well as the bridge response. Data processing included analysis in the time and frequency domains. The results showed that the frequency content of the dynamic wheel loads is distributed over a rather broad band and that the vehicle/bridge interaction is a rather complicated non-stationary process. The basic characteristics of the interaction process can nevertheless be explained with the help of a rather simple two-degree-of-freedom model. Subsequent more detailed analysis consisted of considering an MDOF-model for the bridge and of dividing the analysis range into three parts according to the bridge spans.

1. THE BRIDGE

The Deibüel Bridge is a one-cell prestressed concrete box girder, continuous over three spans of roughly 32, 41 and 37 m length and 11.75 m wide (Fig. 1). Sinusoidal excitation with a servohydraulic vibration generator yielded among other factors the natural frequencies of the three lowest longitudinal bending modes $f_1 = 3.03$ Hz, $f_2 = 4.28$ Hz and $f_3 = 5.49$ Hz [2]. Comparison with calculations showed that the bridge is not behaving as a three-span continuous girder but as a frame with clamped-in columns and horizontally (in the longitudinal direction) fixed bearings at the abutments. The theoretical static boundary conditions as given in Figure 1 do not apply for the practical dynamic loading case of one or more vehicles crossing the bridge. The horizontal force produced under these circumstances e.g. is too small to overcome friction in the PTFE pot-bearings. Hence, the bridge is "horizontally fixed" at the abutments.

This is of special importance because it eliminates the first mode given by a calculation with the condition "horizontally free" at the abutments, $f \approx 2.50$ Hz. Damping of the first bending mode $f_1 = 3.03$ Hz was determined at $\zeta = 0.8\%$ (percentage of critical damping).

Deflection was measured with inductive transducers HBM W20 at several points of the bridge. Only results for the midpoint of the 41 m span, WG 02, and of the 37 m span, WG 22, will be discussed here.

2. THE PAVEMENT

The pavement was intended to have the same longitudinal profile as a section of an existing rough highway with known unevenness ("pavement A"). This was achieved by placing a concrete layer on the bridge deck and using a special copying technique. This technique also allowed the laying of a pavement of equal roughness on an adjacent portion of the

approach. To investigate the influence of pavement unevenness on the behavior of the vehicle on a rigid surface as well as of the vehicle/bridge system, pavement A was smoothed by placing a thin layer of epoxy resin mortar after having performed the first part of the tests. This pavement is referred to as "pavement B". It can be seen from Figure 2 that pavement A was smoother than pavement B above all for large wavelengths.

3. THE VEHICLES

The vehicles dealt with in this paper are four two-axle trucks loaded with concrete blocks up to the legally admitted gross weight of roughly 160 kN. The axle spacing was 3.5 m, 4.3 m, 4.7 m and 5.0 m for the vehicles 11R, 12R, 14R and 13R respectively. The letter "R" indicates that all of the vehicles had radial tires. The car body was supported by leaf springs at both axles, additional viscous dampers were installed at the front axle. Figure 3 gives photographs of the vehicles 12R and 14R.

The device used to measure the dynamic wheel loads is shown in Figure 4. It is basically a contactless infrared sensor which measures the distance between axle and pavement surface and hence the tire deflection. Knowing the force/deflection relationship of the tires, the signals from these sensors can be transformed into wheel loads. To ensure the reliability of this measurement method special measures had to be taken to keep the tire pressure constant during the tests.

4. TEST PROCEDURES

The vehicle was driven at constant speed along the center line of the bridge over the approach and structure. The bridge response and the signals from the four wheel load sensors (transferred to the measurement center by a 2.45 GHz radio-telemetry

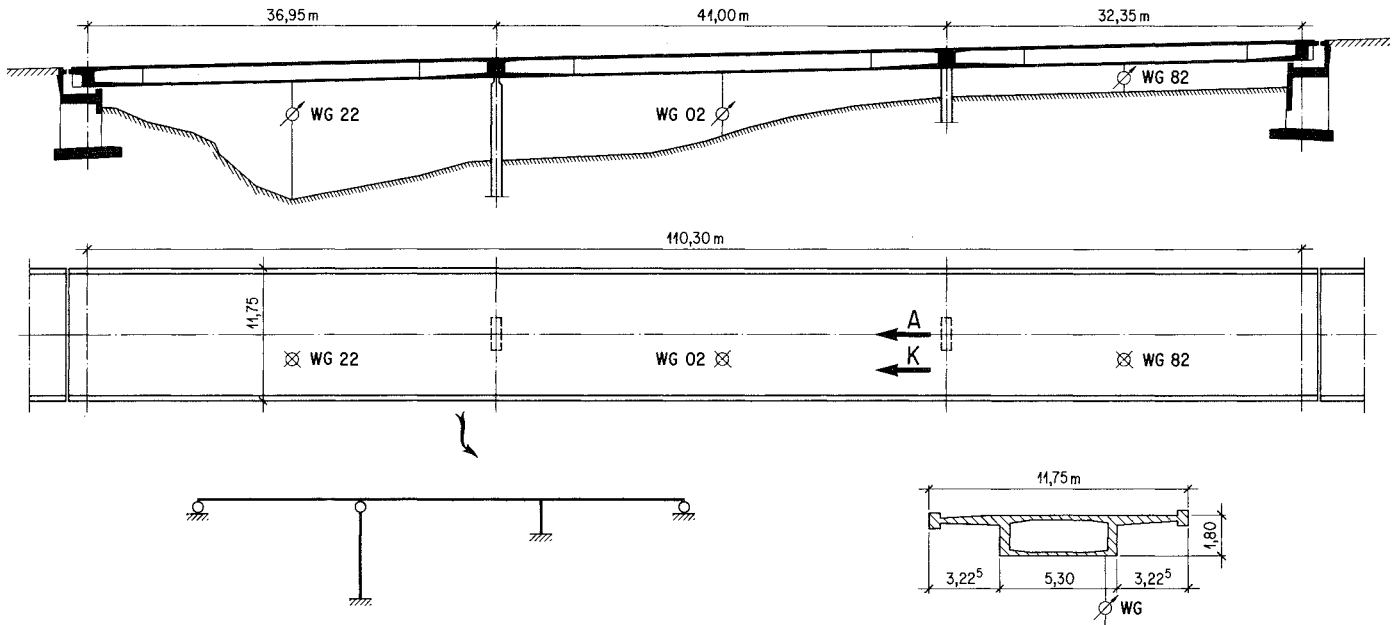


Fig. 1 Geometry and theoretical static system of the Deibüel Bridge. WG 02: Inductive displacement transducer; A: Driving axis.

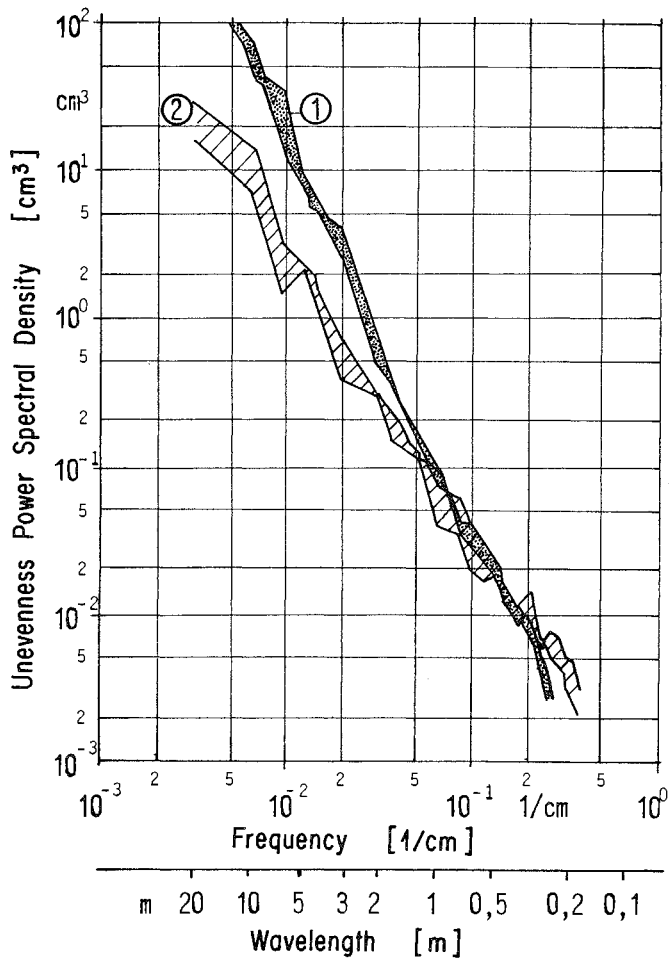


Fig. 2 Unevenness Power Spectral Density of the pavements A (1) and B (2).



Fig. 3 Test vehicles Nr. 12R and 14R (below).

link) were simultaneously stored on magnetic tape. A PCM-system TM/TD8K13 (Johne & Reilhofer) and a Stellavox tape machine were utilized. Test identification consists of the vehicle number, the tire pressure and the pavement: "12R10A" means that the vehicle 12R with a tire pressure of 10 bar was driven over pavement A.

5. TIME DOMAIN ANALYSIS

Data processing in the time domain consisted primarily of the determination of the dynamic increment

$$\phi = \frac{A_{dyn} - A_{stat}}{A_{stat}} \cdot 100 \text{ [%]}$$

with A_{stat} and A_{dyn} being the maximum bridge response under static and dynamic loading with the same vehicle at a given measurement point. Data processing was performed by transferring the measured signals into a Data General Eclipse S130 computer and using Fortran programs. As an example of the results, Figure 5 gives the variation of ϕ with vehicle speed for four two-axle 160 kN vehicles, a tire pressure of 10 bar and pavement A.

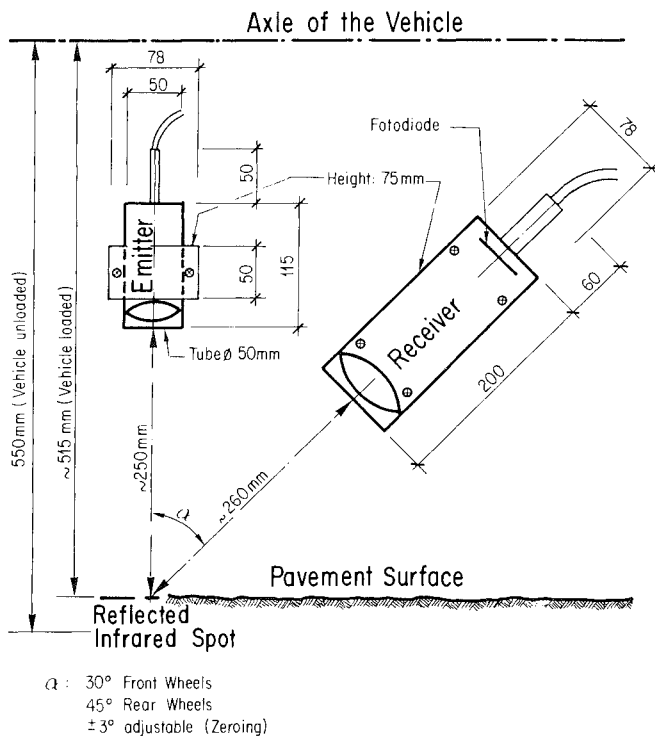
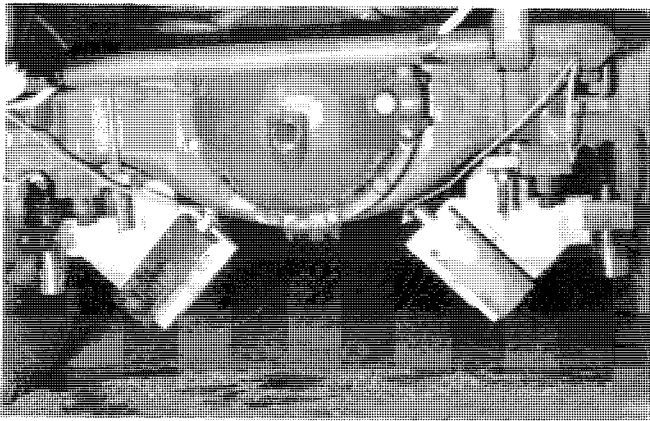


Fig. 4 Measurement of the dynamic wheel load: Principle of operation; the device mounted on the two wheels of a rear axle.

INSTR.	TEST SERIES	ASTAT	PHIMAX[%]	AT v=[km/h]
○	WG Ø2 VEH NR 11	-1.05 MM	40.97	18.2
+	WG Ø2 VEH NR 12	-1.03 MM	45.65	15.1
+	WG Ø2 VEH NR 13	-1.03 MM	52.18	53.9
▲	WG Ø2 VEH NR 14	-1.01 MM	57.10	52.6

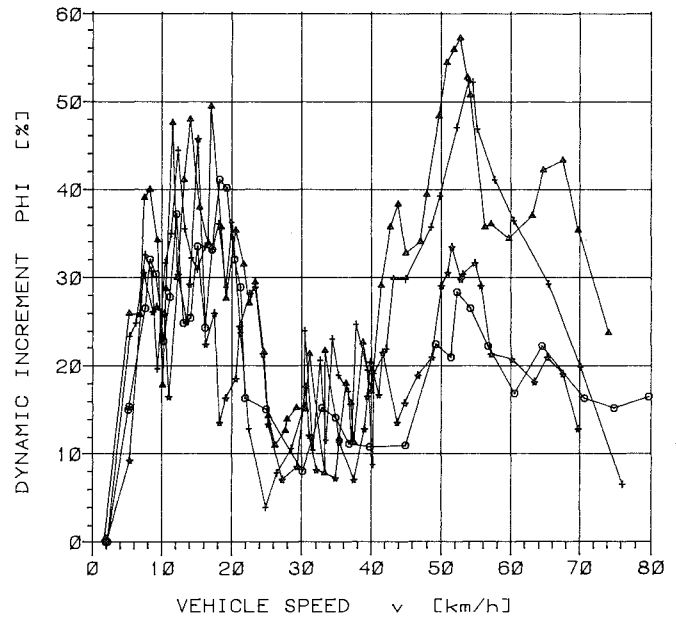


Fig. 5 Dynamic Increments as a function of vehicle speed for two-axle 160 kN vehicles, a tire pressure of 10 bar and pavement A.

6. FREQUENCY DOMAIN ANALYSIS

To determine the behavior of the vehicle on a rigid pavement, the freely vibrating bridge and the system vehicle/bridge during the passage, a modal analysis system was utilized. This consists of an eight-channel DIFA/SCADAS front end with programmable filters and sampling rate, an HP 1000/A700 computer and a software package delivered by LMS, Leuven Measurements & Systems, Leuven, Belgium. The standard application of this system yields the modal parameters of a structure excited by a force $x_i(t)$ at point i and responding with a signal $y_k(t)$ in each measurement point k . The basic data for the calculations are the frequency response functions $H_{ik}(i\omega) = S_{yx}/S_{xx}$ with S_{yx} = cross power spectrum of $y_k(t)$ vs. $x_i(t)$ and S_{xx} = auto power spectrum of $x_i(t)$. For the present application no input signal $x_i(t)$ was available. Therefore, this signal was replaced by an output signal $y_r(t)$ measured at a reference point r . The cross power spectrum $S_{y_r y_k}$ of $y_r(t)$ vs. $y_k(t)$ for every response point k was used instead of the frequency response function H . Phase and amplitude relationships among all of the three bridge and four vehicle signals could thus easily be established.

7. THE VEHICLE ON THE RIGID PAVEMENT

Figure 6 gives an example of the frequency spectra for the four wheel load signals. Relative peaks occur with frequencies between $f = 1$ Hz and $f = 5$ Hz. The highest peak is referred to as "peak frequency". Peak frequencies occur between $f = 1.2$ Hz and $f = 3.2$ Hz. This frequency band is much broader than was assumed from EMPA standard tests. The shape of the vehicle's motion was determined for

14R10A, v = 23.25 km/h

14R10A, v = 63.0 km/h

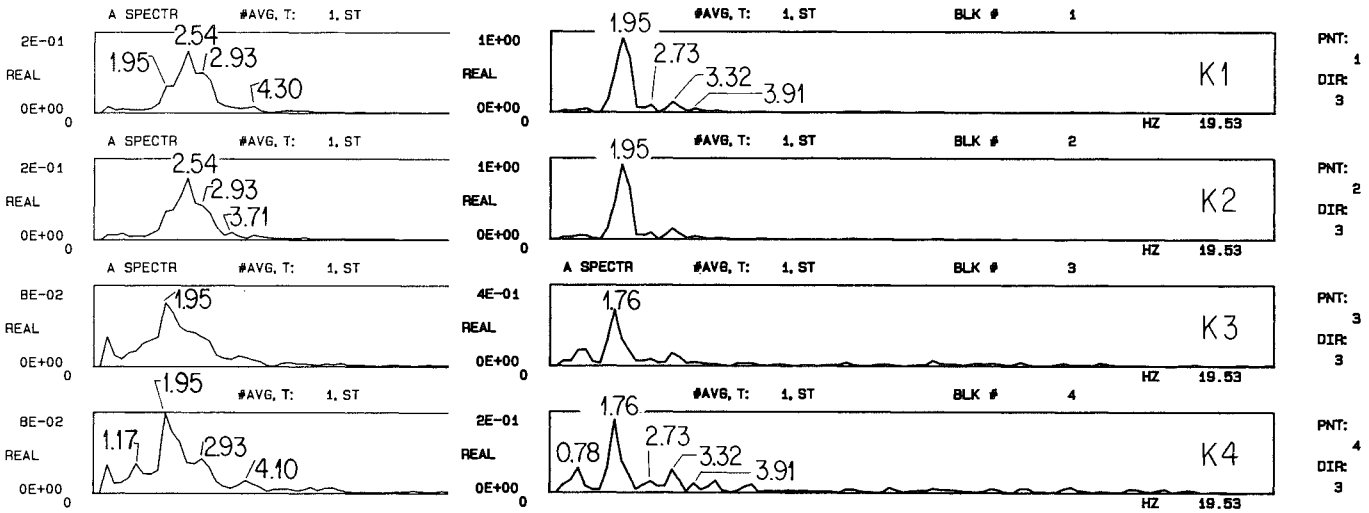


Fig. 6 Examples of auto power spectra of wheel load signals for a moderate and a high vehicle speed. Vehicle 14R, tire pressure 10 bar, pavement A. Frequency resolution $\Delta f = 0.125$ Hz and $\Delta t = 0.25$ Hz respectively. Peak frequencies are indicated. K1 to K4: Rear left, rear right, front left and front right wheel.

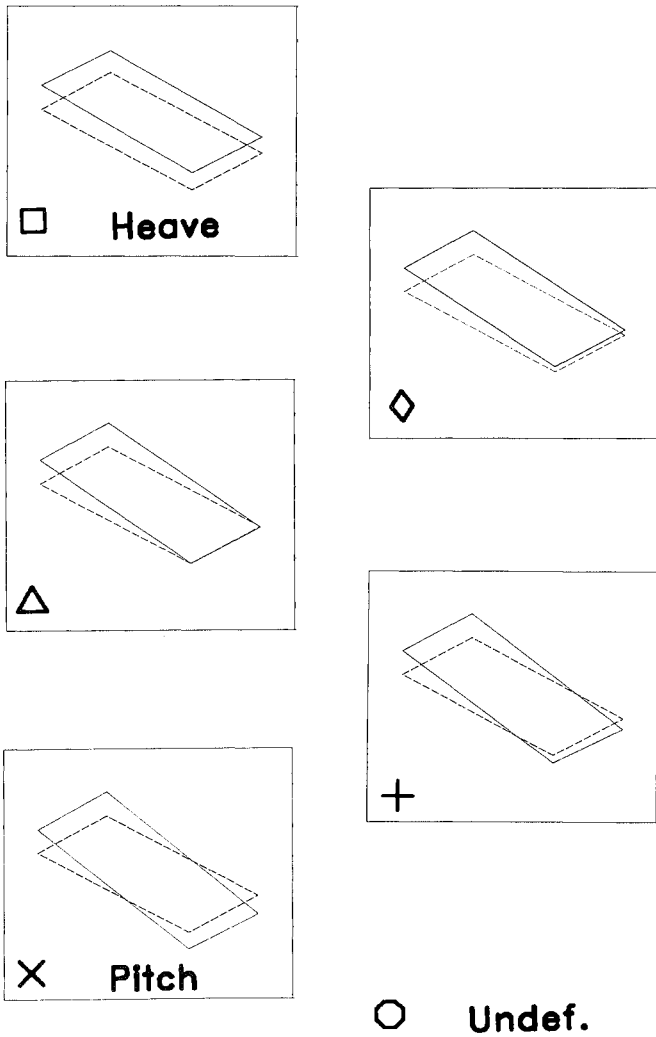


Fig. 7 Vehicle mode shapes. The five modes shown cover about 90% of all shapes observed. "Undefined" mode shapes are indicated with a circle symbol.

relative and absolute peaks with the help of the modal analysis system. This showed that in 90% of all cases the vehicle mode shape is equal to one of the five shapes between pure heave and pure pitch motion given in Figure 7. The "digitized" frequency spectra for rear axles are plotted against vehicle speed in Figure 8. The vehicle mode shapes are indicated with a symbol, the peak frequencies are linked with a solid line. Taking into account the results for both front and rear axles but only for the peak frequencies simplifies the discussion (Fig. 9).

The behavior of the vehicle with increasing speed can be divided into three parts. Region I: The peak frequency is between 2.5 Hz and 3.5 Hz, no mode shape is predominant. Region II: The peak frequency decreases to $f = 2.5 \dots 2.0$ Hz, mode shapes of heave type are predominant. Region III: The peak frequency reaches values of $f \approx 1.5$ Hz and then increases again to $f = 2.0 \dots 2.5$ Hz, only pitch motions occur.

This behavior can be interpreted as follows: In Region I, the suspension leaf springs are blocked and the vehicle vibrates on its tires only. In Region II, the leaf springs are more and more activated and in Region III, this activation is complete. The increase of frequency during Region III may be due to the progressive stiffness of the fully activated leaf springs.

It may be noted that the boundaries between the various regions are not the same for front and rear axles: Front axles always reach the next higher region at a lower speed than rear axles. This may be due to the fact that the force to activate a leaf spring is smaller for front axle springs than for rear axle springs. In addition, these boundaries clearly depend on pavement roughness: For the rear axles and the rough pavement A, these boundaries are $v = 25 \dots 30$ km/h for Regions I/II and $v = 50$ km/h for Regions II/III. A Region II does not exist for the smooth pavement B. The boundary occurring at $v = 50$ km/h therefore separates Region I from Region III in this case.

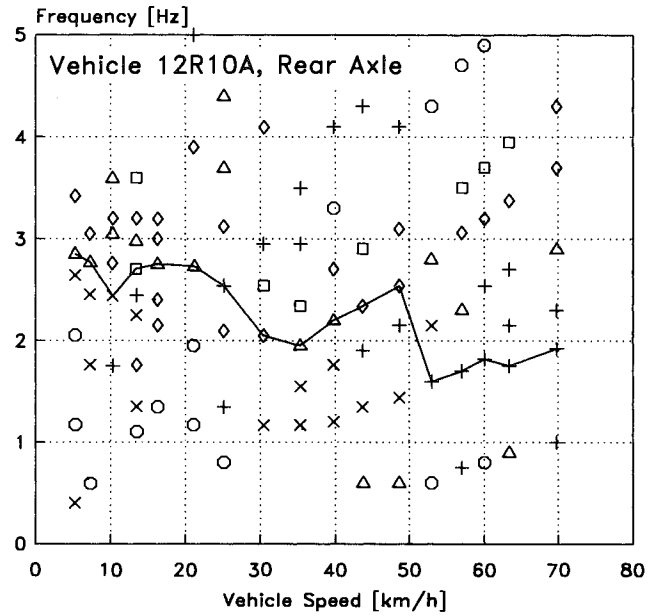
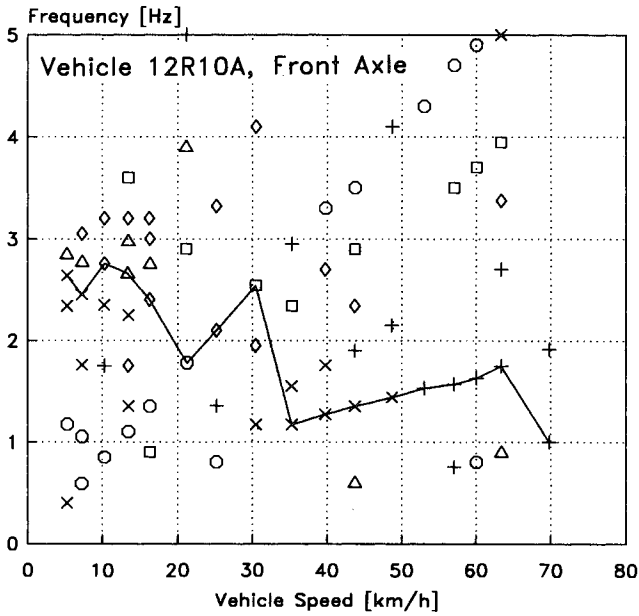


Fig. 8 "Digitized" wheel load spectra versus vehicle speed. The peak frequencies are connected with a solid line. The symbols give the vehicle mode shape according to Figure 7.

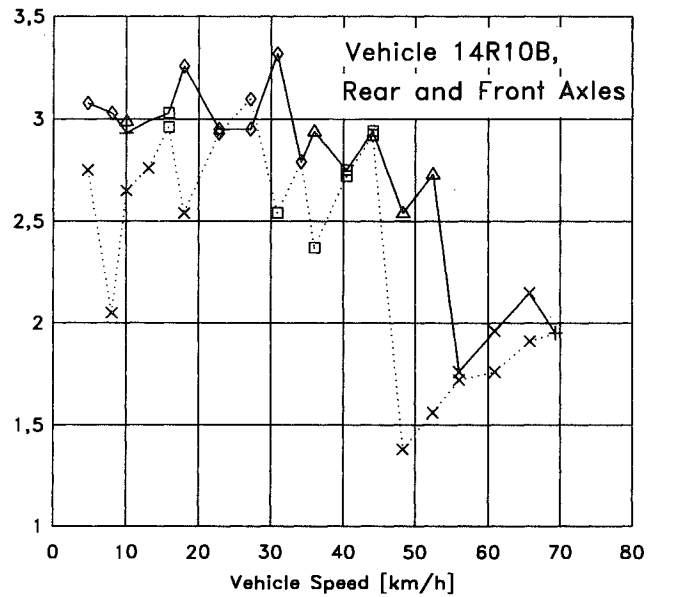
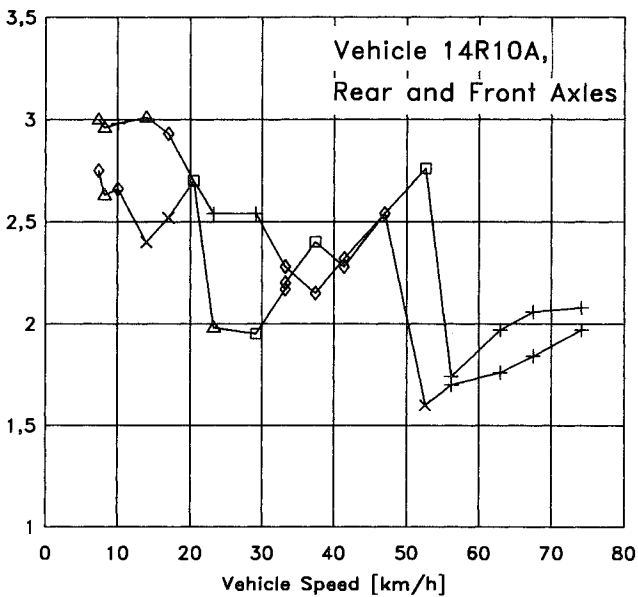
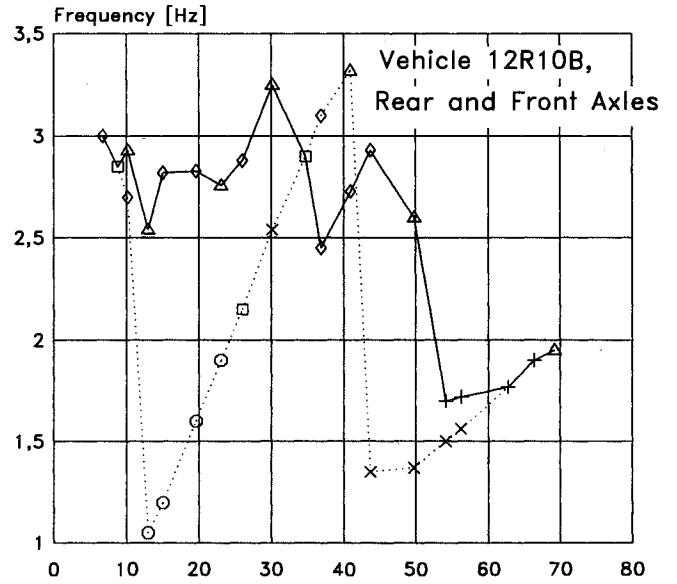
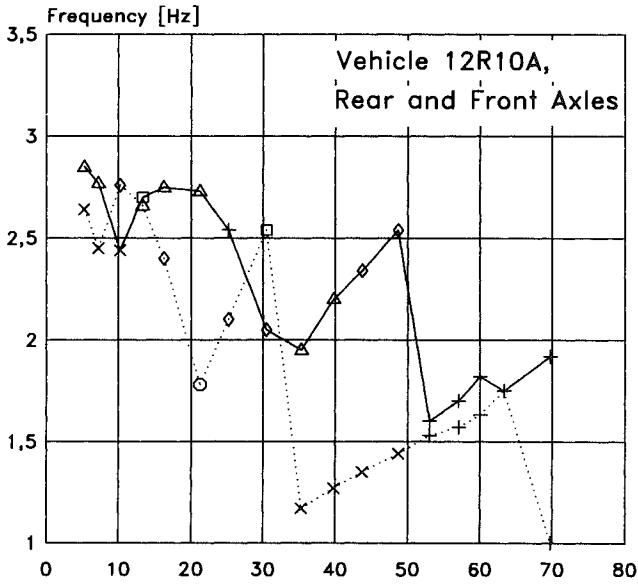
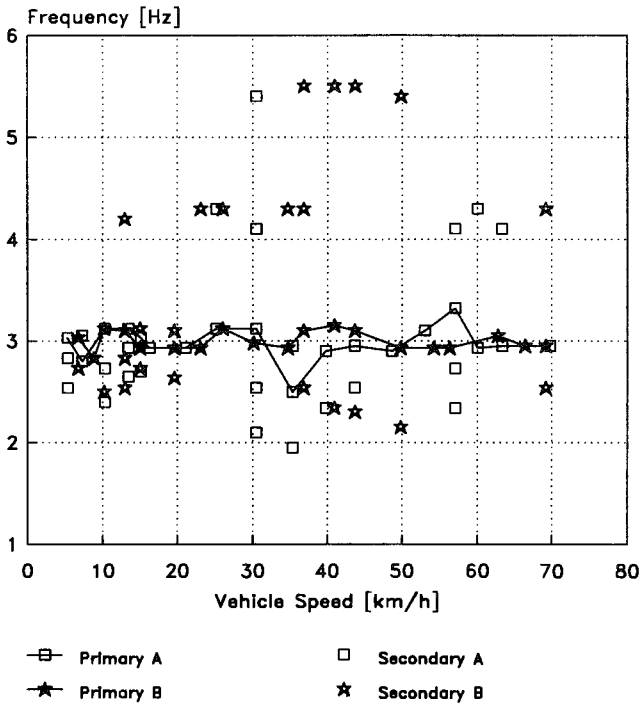


Fig. 9 Peak frequencies and mode shapes versus vehicle speed for front (dotted line) and rear (solid line) axles.

Bridge Response Peakfrequency
Vehicles 12R10A/12R10B, WG 02



Bridge/Vehicle Interaction Peakfrequency
Vehicles 12R10A/12R10B, WG 02

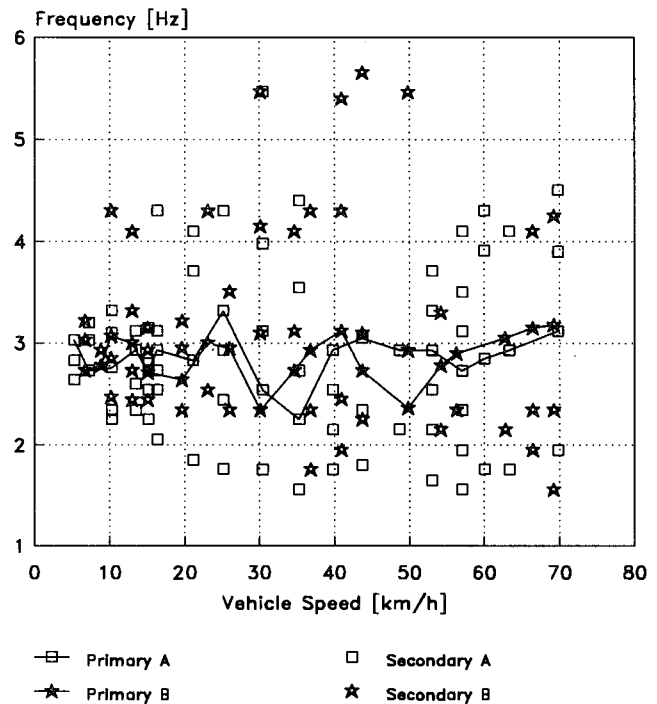


Fig. 10 Peak response frequencies of the loaded bridge.

Fig. 11 Vehicle/bridge interaction peak frequencies.

8. THE VEHICLE ON THE BRIDGE

The behavior of the vehicle during its passage over the bridge is basically the same as over the rigid pavement. Bridge vibrations do not seem to influence the motion of the vehicle in a significant manner.

9. THE FREELY VIBRATING BRIDGE

Frequency domain analysis shows that the first three natural vibrations of longitudinal bending are excited by the vehicle to a greater or lesser extent. The relative magnitude of these modes depends on the measurement point and on vehicle speed. The first mode $f_1 = 3.03$ Hz usually dominates. An example of the importance of higher modes for the bridge behavior is given later (see Paragraph 14).

10. THE VIBRATIONS OF THE LOADED BRIDGE

It can be seen from Figure 10 that the peak frequency of the bridge response mainly varies in a range of $\Delta f = \pm 0.2...0.3$ Hz around the fundamental frequency $f_1 = 3.03$ Hz.

11. VEHICLE/BRIDGE INTERACTION

The cross power spectrum for wheel load vs. bridge response is used here to indicate the intensity of frequency dependent interaction between vehicle and bridge. A similar observation as for the spectra of the bridge response can be made for the peak frequencies of the interaction spectra: They occur in a range of $\Delta f = \pm 0.2...0.3$ Hz on both sides of the bridge natural frequency $f_1 = 3.03$ Hz, on the lower side Δf even reaches values of up to 0.7 Hz (Fig. 11). Figure 12 gives examples of vibrational shapes of the vehicle/bridge system.

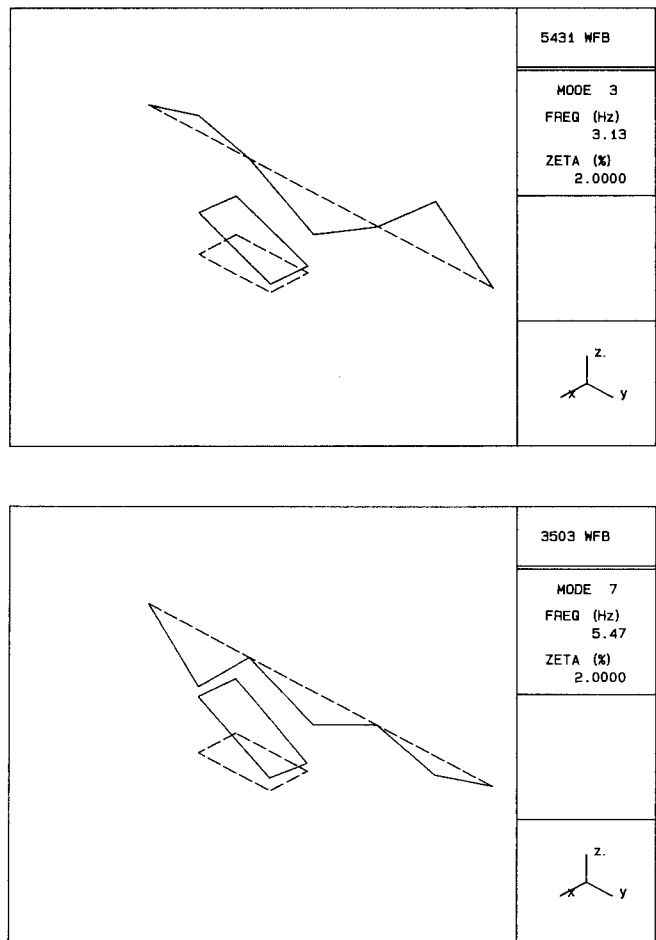
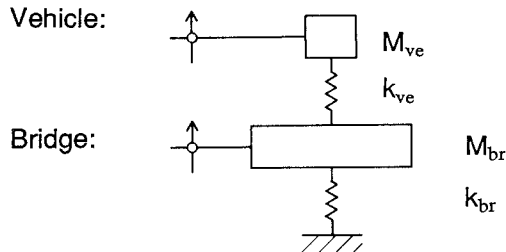


Fig. 12 Vibrational shapes of vehicle/bridge interaction.

12. MODELING

A simple model was sought after in an attempt to explain these frequency variations. It was found that it does not suffice to merely take the vehicle's mass effect into account. This would yield a maximum frequency shift of only $\Delta f = 0.06$ Hz. Investigation of a two-degree-of-freedom system built up by coupling the 1DOF-systems representing the vehicle and bridge respectively yielded a maximum frequency shift of $\Delta f = \pm 0.25$ Hz for the case of equal natural frequencies of the 1DOF-systems (Fig. 13).



The uncoupled 1DOF-Systems with equal natural frequencies:

Bridge: $M_{br} = 442.6 \cdot 10^3$ kg
 $k_{br} = 160.2 \cdot 10^6$ N/m
 $f_{br} = 3.03$ Hz

Vehicle: $M_{ve} = 16.5 \cdot 10^3$ kg
 $f_{ve} = 3.03$ Hz
 $\rightarrow k_{ve} = 6.0 \cdot 10^6$ N/m

The coupled system:

$$(\omega^2)^2 - \left(\frac{k_{br} + k_{ve}}{M_{br}} + \frac{k_{ve}}{M_{ve}}\right) \cdot \omega^2 + \frac{k_{br} \cdot k_{ve}}{M_{br} \cdot M_{ve}} = 0$$

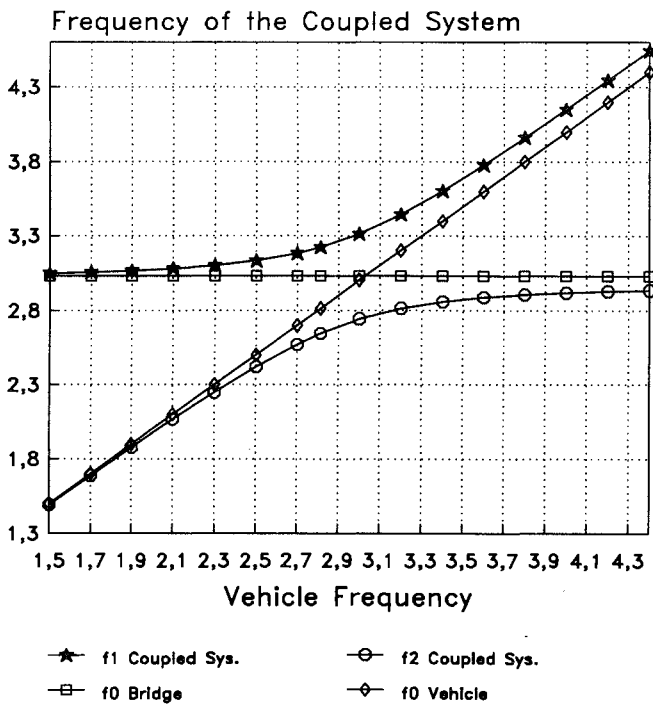


Fig. 13 Modeling of the closely coupled vehicle and bridge as a two-degree of freedom system. Influence of the variation of the vehicles natural frequency on the frequencies of the coupled system (the bridge's natural frequency is constant $f_1 = 3.03$ Hz).

13. DETAILED INVESTIGATION

Further investigations were based on the cross power spectra of bridge response vs. wheel load. The above mentioned model shows that it may not be accurate to extend the data processing range on the process of the vehicle's passage over the bridge as a whole. Therefore, the range was divided into three parts according to the bridge spans. It was also noted that the modal system will always yield a phase angle equal to zero or to π . To investigate the exact phase between load and response in greater detail it was therefore necessary to stop the automatic data processing at the spectrum level and to continue with manual methods.

In addition, an MDOF-model was utilized for the bridge (Fig. 14).

Results of the detailed analysis are presented in Figures 15 and 16. These figures give a) the simultaneously measured time signals of the wheel load K1 and the bridge response WG 02, b) the frequency spectra of the wheel loads K1V and K1W for driving over the approach and bridge respectively, c) the frequency spectra of wheel load K1W and bridge response WG 02 during the vehicle's passage over a given bridge span (calculated from the abovementioned time signals) and d) the cross power spectrum XP of WG 02 vs. K1W.

This cross power spectrum allowed investigation of amplitude and phase relationships between wheel load and bridge response in detail and yielded the basis for the conclusions given below (see [2] for more information).

14. CONCLUSIONS

The most important parameter for the behavior of a bridge span crossed by a vehicle is the relationship between the peak frequency of the dynamic wheel loads and the frequency of the dominating bridge mode. Vehicle/bridge interaction and hence also bridge response are governed by a superposition of the following effects:

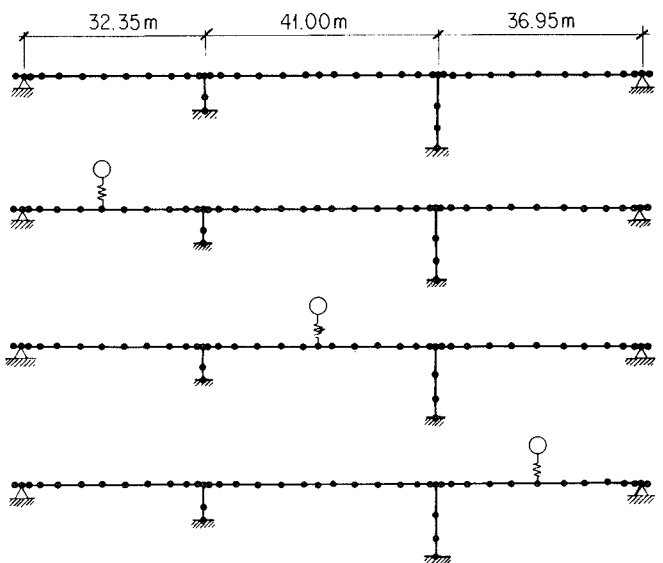


Fig. 14 Modeling of the bridge as an MDOF-system; coupling with the vehicle SDOF-model according to its location on the bridge.

- Close coupling of the vehicle and bridge occurs when their natural frequencies are similar and when the vehicle is near the mid-point of a dynamically significant bridge span. The frequency shift of the resulting in-phase movement of the coupled system is determined by the parameters of the vehicle and bridge as 1DOF-systems. In the case of the Deibüel Bridge, a vehicle mass of 3% of the bridge mass caused a shift of $\Delta f = \pm 0.25$ Hz.
- No coupling occurs when the vehicle is passing over supports (or when the above mentioned frequencies differ significantly from each other).
- During these phases of decoupling, the bridge will store energy in its fundamental modes.
- When the vehicle passes over the second or third span, a superposition of vibrations occurs corresponding to both the coupled and uncoupled states. As the frequencies of these vibrations are relatively close together this results in a beating phenomenon of considerable intensity (Fig. 15). Large dynamic increments occur when the maximum beating amplitude coincides with the maximum static deflection of the bridge.

- All bridge modes with frequencies $f = 1...5$ Hz have to be taken into consideration. For the Deibüel Bridge, the significant decrease in the dynamic increment for $v = 25...30$ km/h (Fig. 5) is due to the fact that the wheel load frequency reached values of $f = 2$ Hz here and therefore excited not only the first but also the second bridge mode ($f_2 = 4.28$ Hz; see Fig. 16).

REFERENCES

[1] Cantieni, R., Dynamic Load Tests on Highway Bridges in Switzerland - 60 Years Experience of EMPA. EMPA Report 211 (1983), Swiss Federal Laboratories for Materials Testing and Research, Dübendorf, Switzerland

[2] Cantieni, R., Beitrag zur Dynamik von Strassenbrücken unter der Überfahrt schwerer Fahrzeuge. Diss. ETH Nr. 9505 (1991);
English Translation: Dynamic Behavior of Highway Bridges under the Passage of Heavy Vehicles. EMPA Report No. 220 (1992)

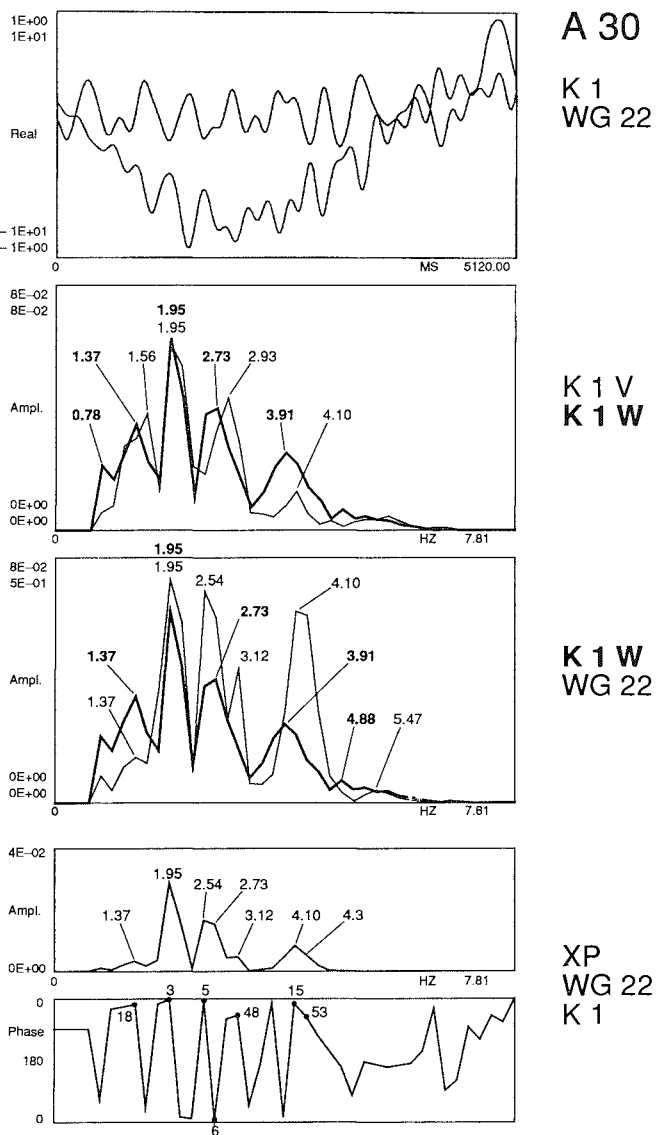
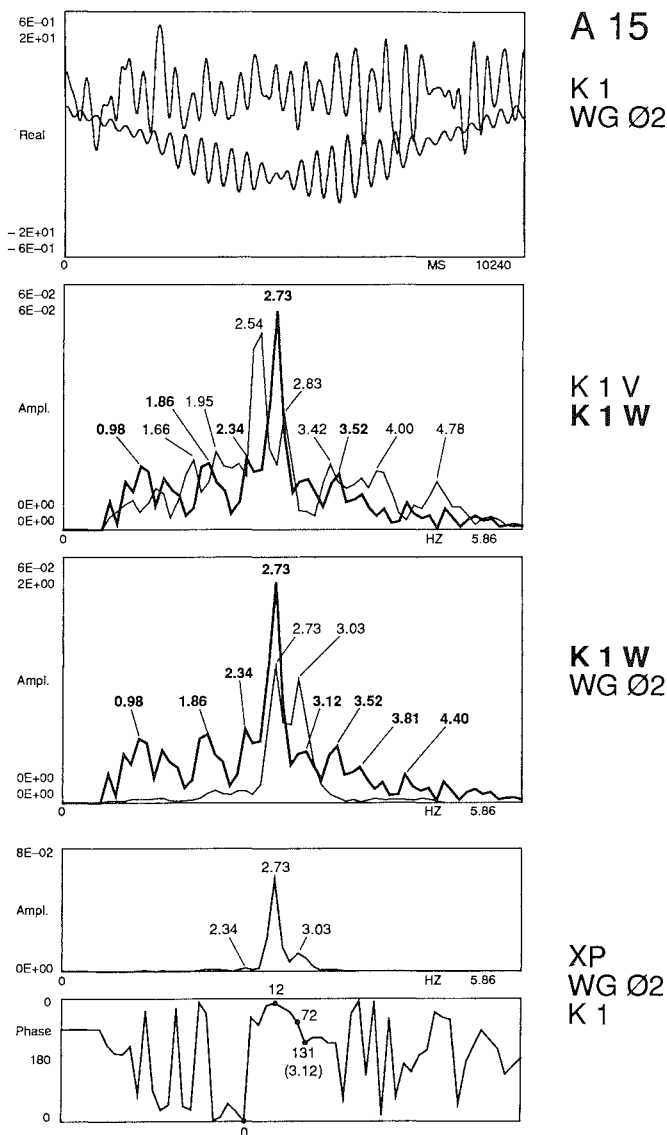


Fig. 15 Vehicle 12R10, Pavement A, $v = 15$ km/h, WG 02 = bridge deflection in the 41 m span, K1 = left rear wheel load. (see paragraph 13 for the detailed description of the diagrams shown.)

Fig. 16 Vehicle 12R10, Pavement A, $v = 30$ km/h, WG 22 = deflection in the 37 m span, K1 = left rear wheel load (see paragraph 13 for the detailed description of the diagrams shown).